Journal of Surgery
Oberman K, et al. J Surg 7: 1672
www.doi.org/10.29011/2575-9760.001672
www.gavinpublishers.com
Research Article

# J147 is Effective in Prevention of Postoperative Cognitive Dysfunction in a Rat Model

**K. Oberman[1*], B.L. van Leeuwen[2], J.E. Villafranca[3], R.G. Schoemaker[1,4]**

[1]Department of Molecular Neurobiology, GELIFES, University of Groningen, Groningen, the Netherlands

[2]Department of Surgery, University Medical Center Groningen, Groningen, the Netherlands

[3]Abrexa Pharmaceuticals, San Diego, United States of America

[4]University Medical Center Groningen, Groningen, the Netherlands

[*]**Corresponding author:** Klaske Oberman, Department of Molecular Neurobiology, GELIFES, University of Groningen, Nijenborgh 7, 9747 AG Groningen, The Netherlands

**Citation:** Oberman K, van Leeuwen BL, Villafranca JE, Schoemaker RG (2022) J147 is Effective in Prevention of Postoperative Cognitive Dysfunction in a Rat Model. J Surg 7: 1672. DOI: 10.29011/2575-9760.001672

**Received Date:** 05 December, 2022; **Accepted Date:** 13 December, 2022; **Published Date:** 16 December, 2022

## Abstract

Postoperative Cognitive Dysfunction (POCD) is a major complication after surgery. Although a dysregulated inflammatory response is indicated to play a key role in POCD, efficacy of anti-inflammatory treatment remains poor. J147 is a newly developed anti-dementia drug that combines neuroprotective, anti-inflammatory and metabolism improving properties. Aim of the present study was to assess the therapeutic potential of J147 in our rat model for POCD. After major abdominal surgery, male (12 weeks old) Wistar rats were divided into: control surgery; surgery treated with acute J147 (gavage before surgery) and surgery treated with chronic J147 (J147 in food). Non-surgery rats served as controls. Timed blood samples were collected to measure peripheral inflammation. Behavioral testing was performed to obtain effects on mood and cognition. At sacrifice, 14 days after surgery, brain tissue was collected to measure neuroinflammation, neurogenesis and cell metabolism. Chronically J147 treated rats lost significantly less body weight after surgery. Moreover, these rats showed preserved short-term (novel location recognition test) as well as long-term spatial memory (Morris Water Maze). However, chronic J147 did not affect peripheral inflammation, indicated by plasma IL-1beta and neutrophil gelatinase-associated lipocalin levels; nor neuroinflammation, indicated by microglial activity; nor neurogenesis or metabolic parameters (AMPK and rpS6 ratio's). Acute J147 did not affect behavioral parameters, neuroinflammation or metabolic parameters.

In conclusion, data show that chronic, but not acute, treatment with J147 can prevent cognitive impairment following abdominal surgery in our POCD rat model, potentially providing a promising new therapeutic avenue for POCD. The lack of impact on markers of (neuro)inflammation, cell metabolism and neurogenesis indicated that J147 may have acted through different, yet to investigate, neuroprotective mechanisms.

**Keywords:** Cell metabolism; Cognition; Inflammation; J147; Neuroinflammation; Postoperative cognitive dysfunction (POCD)

**Abbreviations:** AMPK: Amp-Activated Protein Kinase; AUC: Area Under The Curve: BLA: Basolateral Amygdala; CA: Hippocampal Cornu Ammonis: CSF: Cerebrospinal Fluid; DCX: Doublecortin X: DHC: Dorsal Hippocampus; IBA: Ionized-Binding Adaptor Protein: MWM: Morris Water Maze; NGAL: Neutrophil Gelatinase-Associated Lipocalin; NLR: Novel Location Recognition; NOR: Novel Object Recognition: OF: Open Field; POCD: Postoperative Cognitive Dysfunction; PFC: Prefrontal Cortex; Rps6: Ribosomal Protein S6

### Background

A major complication in patients undergoing surgery is declined cognitive functioning. This often-overlooked

complication is called Post-Operative Cognitive Dysfunction (POCD) [1]. The prevalence of POCD can rise to 37%, depending on age, pre-operative health and the severity and duration of the surgical procedure [2-5]. Patients with POCD display deficits in memory, information processing, concentration and executive functions [1,6]. POCD can have a great impact on the quality of life of both the patients as well as their family and caretakers. However, a lack of understanding of the underlying mechanism hampers the development of effective therapeutic interventions. Evidence indicates that derailed inflammatory responses may play a key role in the disease process [7-12]. Local inflammation, necessary for post-surgical wound healing, can lead to peripheral inflammation [7, 13-15], which is reflected in the brain by microglial activation and production of pro-inflammatory cytokines, resulting in neuroinflammation [7,16-18]. Neuroinflammation could impair neuronal function and lead to a reduced cognitive performance [19,20]. Although there is ample evidence for the role of inflammation in the pathophysiology of POCD, anti-inflammatory interventions, though promising in experimental [20-23] and clinical studies [24-26] have not reached clinical practice so far.

Hovens et al [27] developed an animal model for POCD, indeed showing an inflammatory response after the surgical procedure resulting in increased circulating inflammatory markers, reflected in the brain as neuroinflammation. Moreover, they showed that clinically defined risk factors for POCD, such as advanced age and presurgical conditions, were associated with more wide-spread cognitive decline and exaggerated neuroinflammation [4,28]. These results are in accordance with literature [16,29-31]. Therefore, this rat POCD model seems to provide a clinically relevant model to study potential therapeutic approaches. Although the indicated role of a derailed inflammatory response to surgery in the development of POCD would justify the search for effective anti-inflammatory therapy, inhibition of peripheral inflammation may not be enough to recover cognitive impairment, as shown in a model of POCD after bile duct ligation [32]. Moreover, the observation that standard anti-inflammatory treatment with ibuprofen in the rat model [33] improved cognitive performance and hippocampal neurogenesis, but this promising effect was associated with increased rather than decreased microglia activity, supports the complexity of the condition. A potentially successful treatment may combine the appropriate management of (neuro)inflammation with other neuroprotective effects. A promising compound in this regard could be J147. J147 was shown to be neuroprotective in the central nervous system and in most common age-associated neuropathy models [34-36]. Initially developed as an anti-Alzheimer's disease drug, J147 improved synaptic function, reduced inflammation and oxidative stress markers, improved dendritic structure, and improved cognitive performance [35,37,38]. J147 promotes cell survival and reduces specific changes associated with age [35,39-41] by interaction with ATP synthase [35]. Moreover, J147 was also found to have beneficial effects in other diseases, such as diabetes and depression [35,42-45]. As J147 has been successful in animal models, it is currently in Phase I clinical trials (NCT03838185), supporting a potential future role in anti-dementia treatment. The broad anti-aging and anti-dementia properties of J147 [35], provide support for J147 as a promising new therapeutic agent for POCD. Our rat model for POCD would have the advantage over genetic disease models, in that the time course of disease development is strictly determined by the moment of surgery, facilitating optimal association between the time course of disease development and the intervention. The aim of the present study was to explore the therapeutic potential of J147 to prevent POCD in our rat model. Therefore, effects of acute as well as chronic J147 treatment were investigated in rats that develop POCD after abdominal surgery [27], regarding post-operative cognitive performance, inflammation, neuroinflammation, cell metabolism and neurogenesis.

## Methods

### Rats and Housing

A total of 60 male 12 weeks old Wistar rats (Wu-Wistar) were obtained from Envigo (The Netherlands). Rats were housed in groups of 2-3 individuals and habituated to the animal facility for at least 2 weeks before the start of the experiment. Rats were kept in a climate-controlled room (temperature of 20+/- 2 degrees and humidity of 50% +/- 10%) at reversed light: dark cycle 12:12, with lights off at 9:00 A.M. Water and food (Teklad 2018, Envigo, the Netherlands) were available at libitum. After surgery, rats were housed in individual cages (45cm x 30cm x 50cm). Approval of experimental procedures were given by the National Competent Authority (CCD) and the animal and welfare committee of the University Groningen, the Netherlands.

### Experimental Design

The experimental design is presented in Figure 1. Based on body weight (aimed at 350g at start), rats were randomly assigned to four experimental groups: including non-surgery; control surgery; surgery + acute J147; and surgery + chronic J147. Half of the non-surgery and control surgery groups received vehicle gavage 4-5 hours before surgery, to evaluate effects of gavage per se, and served as control for acute oral treatment. For chronically treated rats, regular food was replaced by J147 containing food from one week before surgery onwards. The other half of the non-surgery and control surgery rats remained on control food and served as controls for the chronically treated rats. Rats were subjected to abdominal surgery and were equipped with a permanent jugular vein catheter for timed blood sampling, as described before in detail [27]. After surgery, rats were housed individually. Control non-surgery rats were brought to the surgery room, were control handled and placed in individual cages as well. In surgery rats,

blood samples were collected from the jugular vein catheter, 1, 6 and 24 hours after surgery. During the first week after surgery, rats were weighed daily and food intake was measured at the last hour of the light period. Between post-operative day 7 and 11, rats were subjected to behavioral testing regarding general exploratory behavior and cognitive performance. Exploratory and anxiety behavior were assessed in the open field test (OF). Short-term spatial memory and object memory were assessed by the Novel Location Recognition (NLR) and novel object recognition (NOR) tests, respectively. Long-term spatial learning, spatial memory and cognitive flexibility were tested in the Morris Water Maze (MWM). On post-operative day 14, the rats were sacrificed, blood samples were collected by cardiac puncture, Cerebrospinal Fluid (CSF) was collected, and brain tissue was collected and processed for immunohistochemistry or molecular analyses.

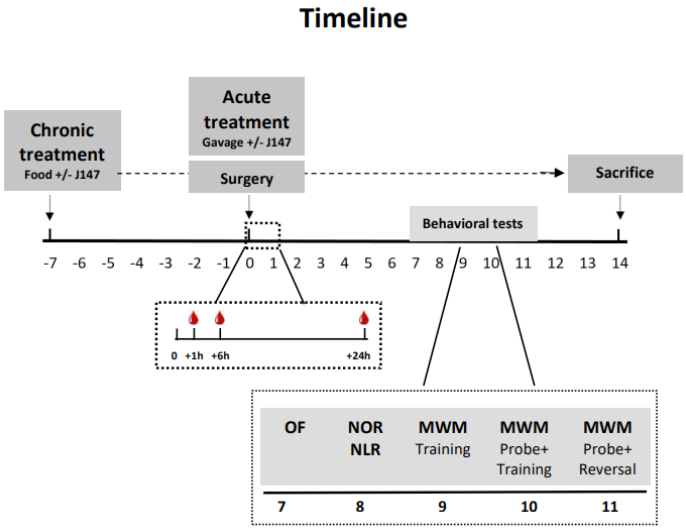


**Figure 1:** Outline of study: Male Wistar rats (n=60) were randomly divided into four experimental groups; non-surgery (n=15), control surgery (n=15), surgery + acute J147 (gavage 20mg/kg, single dose, n=15) and surgery + chronic J147 (food pallets estimating 30 mg/kg/day, 21 days, n=15). After surgery, timed blood samples were collected. Post-operative day 7-11 effects on behavior were assessed in an open field test (OF), Novel object and novel location recognition test (NOR/NLR) and the Morris Water Maze (MWM) to determine exploratory behavior, object memory, spatial learning and memory, and cognitive flexibility, resp. Rats were sacrificed post-operative day 14.

### J147 Treatment

For acute oral treatment, crystalline J147 was suspended in basis for suspension (Fagron, the Netherlands) 37˚C, at 7 mg/ml, and vortexed until homogenous. On the treatment day, a fresh suspension of 1 ml was prepared 30 minutes before gavage and administered using a flexible gavage tube. Gavage of J147 suspension was provided 4-5 hours before surgery, to reach maximum plasma levels at the time of surgery (pilot data ABREXA, USA). Vehicle-treated control rats received gavage of 1 ml basis for suspension 4-5 hours before surgery. For chronic treatment, rats received J147 in their food. Food containing J147 (500mg/kg in Teklad 2018, Envigo, the Netherlands), was available ad libitum from one week before surgery until the end of the experiment, 14 days after surgery. Estimated food intake was 20g per rat per day, which would then result in approximately 30 mg/kg/day J147. After surgery individual food intake was measured daily during the last hour of the light phase. Control rats received Teklad 2018 food (Envigo).

### Surgery

Abdominal surgery was performed as previously described [27]. Briefly, rats were anaesthetized using sevoflurane (±2.5% in air/$O_2$= 2/1) and received 0.01 mg/kg buprenorphine s.c. at the start of the surgery. A heating blanket was used to preserve body temperature. Intestines were exteriorized and the upper mesenteric artery was clamped for 30 minutes, to mimic this aspect of the procedure in abdominal surgery in patients. Within these 30 minutes, a permanent indwelling jugular vein catheter was placed, for one to match the insertion of a permanent venous line in patients, as well as to allow later timed blood sampling without anesthesia. Post-operatively, the rats were allowed to recover and housed individually.

### Behavioral tests

Behavioral tests were performed in the dark (active) period of the rats, excluding the first and last hour of the dark period, as described in detail before [27]. All behavioral tests were performed under dim light conditions, in a room adjacent to the housing room. Rats were habituated to the behavioral room before the behavioral test. Tests were always performed in the same order; day 7 open field test (OF); day 8 novel location recognition test (NLR) and the novel object recognition test (NOR), in random order; day 9-10 the Morris Water Maze (MWM). Rats were tested in random order. All tests were recorded by EthoVision (Noldus Information Technology, Wageningen, The Netherlands) for later of-line analyses using Noldus software: Observer.

**Open field test:** The open field test (OF) was performed to assess exploratory (locomotor activity) and anxiety behavior [46]. The OF box (100 x 100 x 40 cm) consisted of three areas: the center area (60 x 60 cm), border areas (20 x 60 cm) and corners (20 x 20 cm). At the test, rats were placed in the middle of the box and exploring behavior was recorded for 5 minutes after the rat had crossed one of the lines defining the center area. After the test, the box was cleaned using 70% ethanol and dried before the next trail. Locomotion as well as location of the rat was recorded as distance walked, time in corner, walls and center, and number of visits into the center , and analyzed with Ethovision (Noldus,

the Netherlands). Rearing behavior was determined using Eline Software (University of Groningen, the Netherlands). More time and a higher number of visits in the center area and more rearings were regarded as less anxious behavior, while more distance moved was interpreted as more exploratory behavior.

**Novel object and novel location recognition:** The novel object (NOR) and novel location recognition (NLR) tests were included to assess short-term spatial memory and object memory (Hovens et al. 2014b, Dere, Huston and De Souza Silva 2007). For this test, an open square box (50x50x40 cm) with 2 transparent and two grey walls was used. The day before the test, rats were habituated to the box for 3 minutes. The test consisted of four phases of 3 minutes each: habituation, baseline, novel object recognition, and novel location recognition. Between each phase there was a break of 45 seconds in which the rat remained in the test box. The first phase was performed in an empty box and the rat was allowed to explore for 3 minutes. Subsequently, in the second phase two identical objects were introduced to explore. After this, either one of the familiar objects was relocated to another position; NLR, or one familiar object was replaced by a novel object: NOR. Objects were cleaned with 70% ethanol before each phase. After each test the box was cleaned with 70% ethanol to remove smell cues before entering of the next rat. The time exploring the objects was manually analyzed with Eline Software (University of Groningen, the Netherlands). Baseline exploratory behavior was calculated as the time the rat spent exploring both of the objects at phase 2. Novel object preference and novel location preference were calculated as time spent on exploration of the novel or relocated object divided by time spent on exploration of both objects. Results from rats that showed no interest in the objects or only explored one of the two objects in the novel object and novel location test were omitted from further analyses.

**Morris Water Maze:** The Morris water maze (MWM) is representative for long-term spatial learning and memory, and cognitive flexibility [27,47]. The maze entailed a round pool (diameter 140 cm) filled with water of 26±1˚C, which was virtually divided into 4 quadrants. In one of the quadrants an invisible platform (15cm diameter) was submerges 1-2 cm below water level, called target quadrant. Visual cues were placed both inside as outside the pool. The MWM test consisted of six training sessions, two probe trials and three reversal training sessions. The first day consisted of three training sessions. Each training session consisted of three trials, starting at three different quadrants, excluding the target quadrant containing the platform. Rats entered the trials with their nose facing the wall of the pool, and were allowed to find the platform within 60 seconds. If the rat reached the platform, it remained there for 10 seconds before taking it out of the pool. When the rat did not find the platform within 60 seconds, he was gently guided to the platform and left there for 10 seconds. After the 3 trials the rat was towel dried and placed back in his cage. The period between the training sessions for each rat was at least 2 hours. The second day started with a probe trial to assess early spatial memory. In the probe trial the platform was removed from the pool and the rat was placed in the opposing quadrant to the target quadrant and allowed to swim for 60 seconds. Number of platform crossings and time in target quadrant was measured for the first 15 seconds of the probe trails and were used as long-term memory. One hour after the probe trail, three learning sessions (with the platform present) were performed. A learning curve was constructed from the average latencies to reach the platform per training session. The Area Under the learning Curve (AUC) is used to statistically compare the different groups. On the third day, a second probe trail was performed, followed by three reversal learning sessions. The reversal learning was included to assess cognitive flexibility. In the reversal learning the platform was moved to the opposite quadrant of the target quadrant in the learning sessions. Each session consisting of three trials in which the rat was allowed to find the platform for a maximum of 60 seconds. A reversal learning curve was constructed from the average latencies to reach the platform per training session.

**Sacrifice and Tissue Collection**

Three days after behavioral testing rats were deeply anesthetized with pentobarbital (90 mg/kg) and the heart was punctured to collect blood samples. Cerebrospinal fluid (CSF) was subtracted from the subarachnoid space of the spinal cord between C1 and C7. Subsequently, rats were transcardially perfused with cold saline containing Heparin (2 IE/ml) until the liver discolored. Blood samples were centrifuged for 10 minutes at 1600G, and plasma was collected and stored at -80˚C. Brains were dissected and separated into 2 hemispheres. Out of one half of the brain the hippocampus was dissected, frozen in liquid nitrogen and stored in -80˚C for molecular analysis. The other half of the brain was immersion fixated in 4% paraformaldehyde (PFA) and processed for immunohistochemical analysis.

**ELISA**

Blood samples (500uL) were collected from surgery rats equipped with a jugular vein catheter at 1, 6 and 24h after the surgical procedure and for all rats during sacrifice. Blood samples were centrifuged for 10 minutes at 1600G, and plasma was collected and stored at -80˚C. Plasma Il-1β concentrations were determined using the rat IL-1β ELISA kit (Thermo Fisher Scientific, Invitrogen, USA) according to manufacturer's instructions. Plasma IL-6 levels were measured by a rat IL-6 ELISA kit (Thermo Fisher Scientific, Invitrogen, USA), but no reliable measures could be obtained. Plasma and CSF Neutrophil gelatinase-associated lipocalin (NGAL) concentrations were determined using the rat Neutrophil Gelatinase Associated Lipocalin NGAL ELISA kit (Bioporto Diagnostics, Denmark), according to manufacturer's instructions. Peak NGAL values were analyzed at 6 hours after

surgery (Hovens et al. 2016).

**Immunohistochemical staining**

Half of the brain was immersion fixated in 4% paraformaldehyde (PFA) in 0.1M PBS for 36-39 hours and rinsed for 4 days (8 times) in 0.01 M phosphate buffered saline (PBS, pH 7.4). To protect the brain tissue from freezing damage, brains were dehydrated in 30% sucrose in PBS overnight before freezing with liquid nitrogen, and stored at -80˚C. Brains were cut into 25 µm thick sections and stored free floating in 0.01M PBS + 0,1% Natrium Azide at 4 ˚C. Before staining, free floating sections were pretreated with 0.3% $H_20_2$ (Merck Darmstadt, Germany) for 30 min, to block endogenous peroxidase activity.

**Neuroinflammation:** Neuroinflammation was investigated by visualization of microglia in the Prefrontal cortex (PFC) (Bregma +3.73- +2.52), dorsal hippocampus (DHC) (Bregma-1.92 - -4.44) and Basolateral Amygdala (BLA) (on DHC slices) as previously described by Hovens et al. [27,48]. In short, sections were incubated for 3 days with 1:2500 rabbit-anti IBA-1 (Wako Chemicals, Nuess Germany) in 1% BSA (Sigma-Aldrich, St. Louis MO, USA), 0,1% Triton X-100 (Merck Darmstadt, Germany) at 4˚ and followed by 2 h incubation with 1:500 goat-anti rabbit secondary antibody (Jackson ImmunoResearch, Suffolk, UK). Labelling was visualized using a 0.35 mg/ml DAB (Sigma-Aldrich, St. Louis, MO, USA) solution activated with 0.1% H2O2. All sections were thoroughly rinsed with 0.01M PBS between staining steps. Sections were transferred to glass slides and dehydrated through gradients of ethanol and xylol solutions. Photographs were taken (200x magnification, Olympus BH2 microscope, Leica DFC 365FX camera and Leica LAS software) from the hilus and CA1 region of the hippocampus, the PFC and BLA. Using image analysis software (Image-Pro Plus 6.0), the coverage, density, the average total cell size, processes size and average cell body size of microglia were determined. Neuroinflammation was measured from calculated microglia activity [48]. When microglia become activated, they change their shape from ramified, small cell body with extensive processes, to activated microglia with larger cell body and/or retracted thicker processes [49,50]. The microglial cell body size as percentage of total microglia size was used as a measure of microglial activation [48].

**Neurogenesis:** Neurogenesis was obtained from doublecortin (DCX) staining of dorsal hippocampal sections as described before [27]. In short, sections were incubated for 3 days with 1:1000 goat-anti DCX (Santa Cruz, Dallas, USA) in 3% normal rabbit serum, 0,1% TX at 4 ˚C, followed by incubation with 1:500 rabbit-anti goat secondary antibody (Jackson, Wet Grove, USA) for 2h at room temperature. Sections were incubated for 2 h with avidin-biotin peroxidase complex (Vectastain ABCkit, Vector, Burlingame, USA) at room temperature. Labeling was visualized using a 0.35 mg/ml DAB enhanced with ammonium nickel sulfate solution and activated with 0.1% H2O2. All sections were thoroughly rinsed with 0.01M PBS between staining steps. All dilutions were made in 0.01 M PBS, except for the DAB which was made in MilliQ. Sections were transferred to glass slides and dehydrated through gradients of ethanol and xylol solutions. DCX photos were taken at 40x magnification using Olympus BH2 microscope (Leica DFC 365FX camera and Leica LAS software), imaging the entire dentate gyrus. Pictures were analyzed using Image-Pro Plus software (Version 6, Media Cybernetics, Rockville MD, USA). The area of DCX positive cells per length of the dentate gyrus was considered a measure for neurogenesis.

**Western Blot Hippocampal Tissue**

**Sample preparation:** After sacrifice, hippocampi were frozen in liquid nitrogen and stored at -80˚C. Hippocampi were homogenized in RIPA buffer containing 1:100 Complete protease inhibitor (Sigma Aldrich, Darmstadt, Germany), 1:60 Phosphatase inhibitor cocktail 2 (Sigma Aldrich, Darmstadt, Germany), and 1:50 Phosphatase inhibitor cocktail 3 (Sigma Aldrich, Darmstadt, Germany) followed by bead beating with 1,5 mm glass beads for 3 x 15 seconds (MP biomedicals).

**Lipocalin:** Neutrophil gelatinase-associated lipocalin (NGAL) is an inflammatory marker which is rapidly upregulated under pro-inflammatory conditions. Moreover, it has a multifaceted role in modulating the inflammatory response to infection and injury [51]. As previously shown, NGAL has been associated with cognitive impairment in chronic inflammatory conditions [52] and after surgery [53,54], implicating a potential role for NGAL to connect peripheral and neuroinflammation to the disease pathology of POCD.

Homogenates were centrifuged for 10 min at 14000 g at 4˚C, and supernatant was collected. Total protein concentrations were determined using a Bradford assay in 96-well microplates (CELLSTAR, Greiner Bio-One, Alphen aan den Rijn, the Netherlands) and supernatant was diluted to 1,7 µg/µL in RIPA lysis buffer (ThermoFisher Scientific) and 20% Laemmli sample buffer (50% glycerol, 5% β-mercaptoethanol, 8,3% SDS, 0,008% bromphenol blue in 1 M Tris-HCl). Samples were denaturized for 5 minutes at 95˚C and loaded on a 5% stacking gel. Proteins were separated by gel electrophoresis using a 12% separation gel ($ddH_2O$, 40% Acrylamide mix (Bio-rad), 1.5 M Tris pH, 8.8, 10% SDS, TEMED (Bio-rad), 10% ammonium persulfate (APS)). Thereafter, the PVDF membranes (Sigma Aldrich) were activated 1 minute in methanol, and the proteins were transferred to the membrane using wet blot for 90 minutes at 4˚C in 1x Towbin buffer pH (7.6). Membranes were blocked using 1: Iblock Protein-based blocking reagent (ThermoFisher Scientific) for 1 hour at room temperature, incubated with 1:100 Anti-Lipocalin-2/ NGAL (Ab63929, Abcam) or 1:500.000 Anti-Actin (MP Biomedicals) overnight at 4˚C and incubated with 1:10000 horseradish peroxidase (HPR)-conjugated

Goat-anti-mouse (SantaCruz Biotechnology, Dallas, USA) for detection of β-Actin, and 1:5000 dilution Goat-anti-Rabbit IgG HRP-conjugated (Cell Signaling Technology, Leiden, Netherlands) for detection of NGAL. The Actin bands were developed using 1:1 Standard ECL solution (ThermoFisher Scientific) and NGAL bands were developed using 1:2 Dura ECL (ThermoFisher Scientific). The chemiluminescence was detected using the ChemiDoc (Bio-Rad). Quantitative levels of housekeeping gene protein Actin were used as correction for baseline translation of proteins. Quantitative analysis of NGAL levels were calculated as Area Under the Curve of the Westernblot bands (AUC, Image Lab version 6.1 Bio-rad). NGAL levels in the hippocampus are expressed as NGAL to actin levels.

**AMPK and rpS6:** Previous research showed that J147 can bind to and partially inhibit the mitochondrial alfa-F1 subunit of ATP synthase (ATP5A) and therefore promote cell survival and reduce specific changes associated with age [35,39-41]. To explore whether inhibition of ATP synthase (ATP5A) may play a role in the results of the present study, AMP-activated protein kinase (AMPK) and ribosomal protein S6 (rpS6) were measured in the hippocampus [35]. Homogenates were centrifuged for 10 min at 6000 g at 4˚C, and supernatant was collected. Total protein concentrations were determined using a BCA assay in 96-well microplates (CELLSTAR, Greiner Bio-One, Alphen aan den Rijn, the Netherlands) and supernatant was diluted to 1,7 µg/µL in RIPA lysis buffer (ThermoFisher Scientific) and 25% Laemmli sample buffer (50% glycerol, 5% β-mercaptoethanol, 8,3% SDS, 0,008% bromphenol blue in 1 M Tris-HCl). Samples were denatured for 5 minutes at 95˚C and loaded on a 12% SDS polyacrylamide gels. Proteins were separated by gel electrophoresis and transferred onto PVDF membranes (Millipore). Membranes were blocked with 5% BSA and 0,2% sodium acid for 20 minutes at room temperature, incubated with 1:1000 anti-AMPK/ rpS6/ p-AMPK / p-rpS6 (Cell signaling, rabbit or mouse anti rat) or 1:1000000 anti-actine (mouse anti-rat, ImmunO™, MP Biomedicals) in 5% BSA and 0,1% sodium acid overnight at 4˚C and incubated with (1:4000, Thermo scientific) secondary antibody in 2.5% BSA for two hours at room temperature. Protein bands were visualized by enhanced chemiluminescence (Las400 mini-imager, GE Healthcare Life Science) and quantified using ImageQuant™ (GE Healthcare Life Science) and ImageLab (Bio-Rad) to determine AMPK, p-AMPK, rpS6, p-rpS6 and actin. AMPK, p-AMPK, rpS6 and p-rpS6 values were corrected for actin. Hippocampal p-AMPK to AMPK and p-rpS6 to rpS6 ratios were used as reflection of the cell metabolism.

## Data Analyses

Data are presented as mean ± SEM. Statistical analysis was performed using SPSS (IBM SPSS Statistics, Version 27, Armonk, NY). Area under the Curve (AUC) was calculated using GraphPad Prism version 5 (GraphPad Software, La Jolla California USA). Data that exceeded mean ± twice standard deviation of its group are regarded as outliers and excluded from analyses of comparing means. To assess the effect of surgery, non-surgery and control surgery groups were compared using an independent T-test. As the non-surgery rats appeared to underperform compared to our previous studies [27] in young Wistar rats, to evaluate the effects of interventions, only surgery groups were compared. Group averages of the surgery groups are compared by one-way ANOVA and if significant effects were present, post hoc Dunnet analysis, with control surgery group as control, were used to compare the surgery groups. Spatial learning in the MWM, food intake and bodyweight curves was analyzed using repeated measurements General Linear Model (GLM). Correlations between parameters were obtained by a Pearson correlation. Differences were regarded statistically significant when $p \leq 0.05$. Relevant trends were indicated if $p<0.10$.

## Results

### General

All 60 rats completed the protocol and were included in the study. However, one rat died of unknown cause just before sacrifice. Since no significant effects of vehicle gavage were observed, rats with vehicle gavage and rats on control food were pooled into one non-surgery group and one control surgery group, resulting in the following experimental groups for behavioral analyses: non-surgery control; surgery control; surgery + acute J147 (surgery + acute); surgery + chronic J147(surgery + chronic); n=15 each.

### Body weight and food intake

Rats that were fed the J147 diet, gained on average 32.0 ± 1.8 g during their first week on the diet, which was comparable to 33.5 ± 3.0 g in control fed rats, and suggested no preference or aversion for the diet food. At the time of surgery, non-surgery rats weighed 348 ± 4g; control surgery rat 346 ± 3g; acutely treated rats 347 ± 3g and chronically treated rats 348 ± 3g. All groups that underwent surgery lost significant body weight compared to their start weight (Figure 2A). Chronically treated rats retained a higher body weight during the 5 days post-surgery (Figure 2A), but did not have a higher food intake compared to the other surgery groups (Figure 2B). Chronically, but not acutely treated rats, lost significant less maximum body weight in the 5 days post-surgery than the control surgery rats (Figure 2C). Five days after surgery all rats were back to normal level of food intake of around 22 grams per day (Figure 2B).

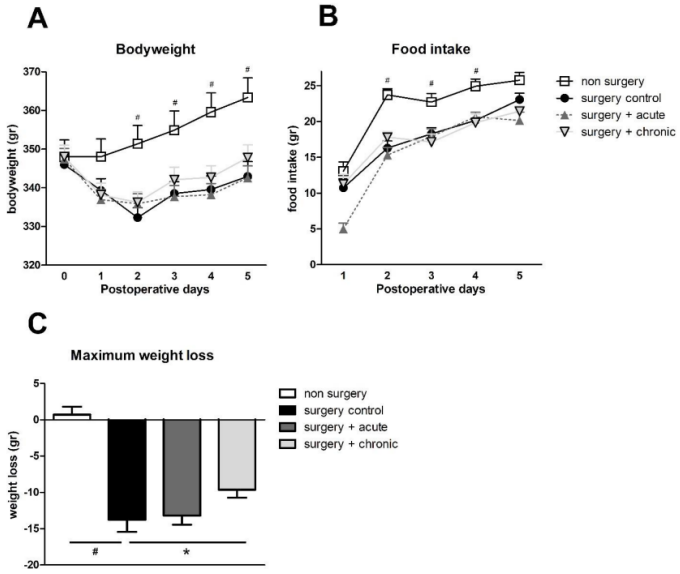


**Figure 2:** Time course of body weight (A) and food intake (B) during the first 5 days post-surgery, as well as maximal weight loss during the first 5 days after surgery(C) in non-surgery (n=14-15), surgery control (n=15), acutely J147 treated (n=14) and chronically J147 treated (n=14) rats. *: significant ($p<0.05$) difference between indicated groups (effect of J147 treatment). #: significant ($P<0.05$) effect of surgery.

## Behavior

**Open field behavior:** The distance moved, measure for exploratory behavior, and percentage of time spend in corner and border, measure for anxiety, in the open field were similar for all groups (Figure 3A and 3D). Whereas location in the open field was not affected in acutely treated rats, chronic J147 treated rats tended to pay more visits to the center ($p=0.12$; Figure 3B) and displayed significantly more rearing behavior compared to control surgery rats (Figure 3C).

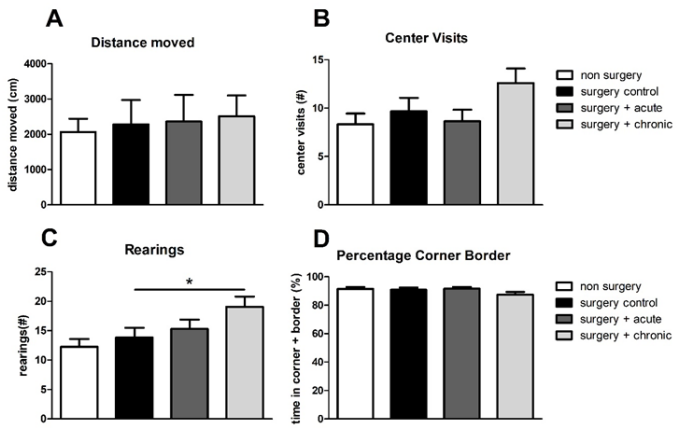


**Figure 3:** Open field behavior (mean ± SEM) in the non-surgery (n=14-15), surgery controls (n=15), acutely J147 treated (n=14-15) and chronically J147 treated (n=14-15) rats. A) distance moved(cm), B) number of center visits), C) number of rearings and D) percentage of time in corners and borders. *: significant ($p<0.05$) difference between indicated groups (effect of J147 treatment).

**Short-term memory:** In the baseline phase of the novel object (NOR) and novel location recognition (NLR), tests taken at 8 days post-surgery, all groups showed similar interest in the objects (on average 20% ±12% of time). Also, no side preference was observed. Data of rats that explored none or only one of the two objects in the NOR or NLR and rats that did not move during the test were excluded from analysis (4 rat from control surgery; one from acutely and 4 from the chronically treated rats). In the remaining rats, object recognition did not differ significantly between groups. In the location preference test, non-surgery and surgery control rats did not perform significantly above chance level, whereas both acute and chronic J147 treated rats did (Figure 4). However, location preference was only significantly improved in the chronically treated J147 rats compared to the control surgery group (Figure 4).

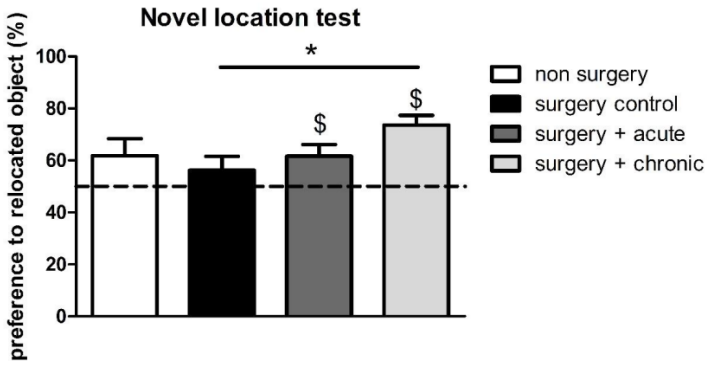


**Figure 4:** Novel location recognition test (mean ± SEM) in the non-surgery (n=9), surgery controls (n=11), acutely J147 treated (n=14) and chronically J147 treated (n=11) rats. $: significant (p<0,05) difference from chance level 50%; dotted line; *: significant (p<0.05) difference between indicated groups (effect of J147 treatment).

**Long-term learning and memory:** The learning curve of the Morris water maze (MWM) showed a significant learning process, with no differences in learning capacity between groups (Figure 5A). In the first probe trail, no difference in spatial memory was seen between the groups (data not shown). However, spatial memory differed significantly between groups in the second probe trail. Control surgery rats showed an impaired long-term spatial memory, reflected in less time in target quadrant and lower number of platform crossings in the probe trail. Moreover, whereas acute J147 treated rats did not show improvement compared to surgery control rats, chronic J147 treated rats showed an improved spatial memory capacity, as they spent more time in the target quadrant and had a higher number of platform crossings (Figure 5B and 5C). The reversal training showed a significant learning process, but no differences in escape latency between groups (AUC control surgery 19.6 ± 1.4, surgery + acute J147 19 ± 1.6 and surgery + chronic J147 19.8 ± 2.1 seconds). Memory consolidation, the difference between latency of the last training session and the first reversal session, was also not significant different between groups (control surgery 11.4 ± 2.7, surgery + acute J147 9.4 ± 2.3 and surgery + chronic J147 12.2 ± 2.8 seconds).

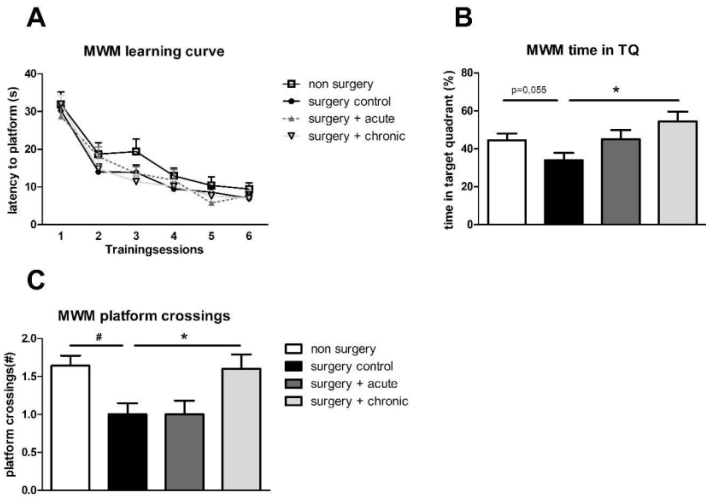


**Figure 5:** Results from the Morris water maze test (MWM) (mean ± SEM) in the non-surgery (n=14-15), surgery control (n=14-15), acutely J147 treated (n=14-15) and chronically J147 treated (n=15) rats. A) Spatial learning in the MWM. Average escape latency is shown for the 6 training sessions (s), B) spatial memory in the MWM. The percentage of time in the target quadrant in the probe trail (%) and C) spatial memory in the MWM. The number of platform crossings in the probe trail (#). *: significant (p<0.05) difference between indicated groups (effect of J147 treatment). #: significant (P<0.05) effect of surgery.

### Neurogenesis

Neurogenesis, measured by DCX-positive young maturing neurons in the hippocampal dentate gyrus, was reduced in the control surgery rats compared to the non-surgery rats. However, this lowered neurogenesis was not affected by either acute or chronic J147 treatment (control surgery: 3.32 ± 0.14; surgery + acute J147: 3.29 ± 0.21 and surgery + chronic J147 3.24 ± 0.20 DCX positive cells per length). Neurogenesis was not significant correlated with either neuroinflammation or cognitive parameters.

### Neuroinflammation

Figure 6 shows the microglial activity in hippocampus (CA1 and hilus area), the Prefrontal cortex (PrL) and de basal lateral amygdala (BLA), calculated as cell body per cell size ratio. In

the control area, the BLA, no significant differences between the groups were observed (Figure 6F). Neuroinflammation induced by abdominal surgery was supported by selectively increased microglia activity in the CA1 area of the hippocampus, but not in the hilus (Figure 6C and 6D). Acute J147 treated animals showed a tendency towards lowered microglia activity in the hilus of the hippocampus and PrL of the prefrontal cortex (Figure 6D, and 6E, p<0,1). However, no significant effect of chronic J147 treatment was seen in the CA1, hilus and PrL (Figure 6C, 6D, and 6E). For the underlying morphological parameters of microglia, no effects were observed between the surgery groups (Table 1), except for the PrL and BLA where the coverage was significant lower in the chronic J147 treated rats than control rats.

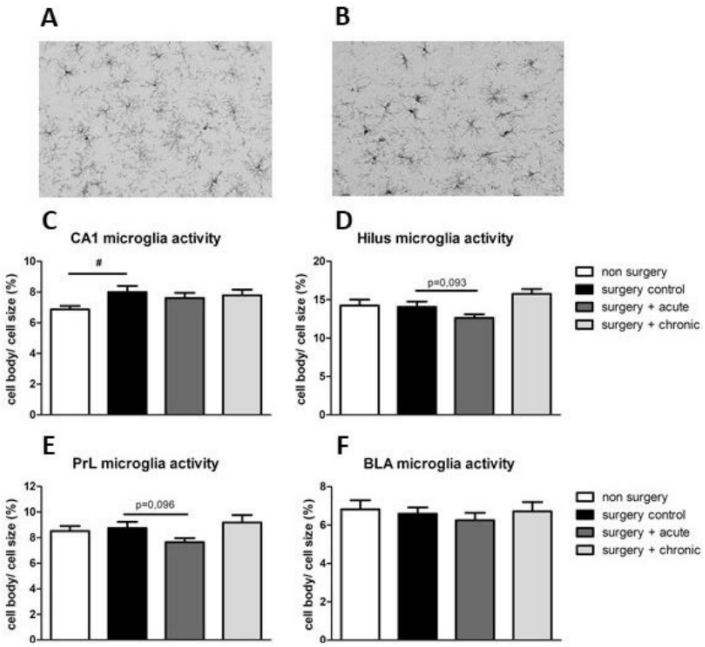


**Figure 6**: Microglia activity in different brain areas (mean ± SEM) expressed in microglia cell body per cell size in the non-surgery (n=14-15), surgery controls (n=13-14), acutely J147 treated (n=14-15) and chronically J147 treated (n=14-15) rats. A) Microscopic picture (200x magnification) of microglia in the Ca1 of non-surgery rats, B) Microscopic picture (200x magnification) of microglia in the Ca1 of surgery control rats, C) Microglia activation in the CA1 region of the hippocampus, D) Microglia activation in the hilus of the hippocampus, E) Microglia activation in the PrL region of the prefrontal cortex and F) Microglia activation in the Basal lateral amygdala (BLA). *: significant (p<0.05) difference between indicated groups (effect of J147 treatment). #: significant (P<0.05) effect of surgery.

| | **Non-surgery** | **Control surgery** | **Surgery + acute J147** | **Surgery + chronic J147** |
|---|---|---|---|---|
| | **CA1** | | | |
| **Density** | 1.27 ± 0.04+ (p=0.098) | 1.39 ± 0.05 | 1.32 ± 0.04 | 1.38 ± 0.07 |
| **Coverage** | 0.13 ± 0.00 | 0.13 ± 0.00 | 0.12 ± 0.01 | 0.12 ± 0.01 |
| **Cell size** | 10193 ± 353 | **8852 ± 413#** | 9136 ± 528 | 8599 ± 473 |
| **Cell body size** | 680 ± 22 | 701 ± 20 | 705 ± 21 | 712 ± 23 |
| **Dendrite size** | 9496 ± 340 | **8389 ± 384#** | 8852± 446 | 8524 ± 380 |
| | **Hilus** | | | |
| **Density** | 3.17 ± 0.15 | 3.27 ± 0.15 | 3.16 ± 0.14 | 3.35 ± 0.07 |
| **Coverage** | 0.12 ± 0.00 | **0.13 ± 0.00#** | 0.13 ± 0.00 | 0.13 ± 0.00+ (p=0.076) |

| | | | | |
|---|---|---|---|---|
| **Cell size** | 4100 ± 205 | 4063 ± 155 | 4453 ± 208 | 3886 ± 143 |
| **Cell body size** | 596± 210 | 567 ±15 | 553±15 | 574 ± 16 |
| **Dendrite size** | 3499 ± 196 | 3492 ± 156 | 3900 ± 201+ (p=0.086) | 3297 ± 139 |
| | **PrL** | | | |
| **Density** | 1.41 ± 0.04 | 1.44 ± 0.07 | 1.29 ± 0.05 | 1.37 ± 0.08 |
| **Coverage** | 0.12 ± 0.01 | 0.13 ± 0.00 | 0.13 ± 0.00 | **0.11 ± 0.00*** |
| **Cell size** | 8799 ± 405 | 8904 ± 612 | 9944 ± 413 | 8200 ± 465 |
| **Cell body size** | 731 ± 12 | 748 ± 17 | 724 ± 21 | 732 ± 16 |
| **Dendrite size** | 8056 ± 398 | 8160 ± 602 | 9220 ± 410 | 7467 ± 461 |
| | **BLA** | | | |
| **Density** | 2.07 ± 0.09+ (p=0.086) | 2.30 ± 0.10 | 2.33 ± 0.08 | 2.23 ± 0.11 |
| **Coverage** | 0.15 ± 0.00+ (p=0.099) | 0.16 ± 0.01 | 0.16 ± 0.01 | **0.14 ± 0.00*** |
| **Cell size** | 7078 ± 360 | 6836 ± 270 | 6910 ± 268 | 6695 ± 297 |
| **Cell body size** | 469 ± 27 | 458 ± 20 | 427 ± 27 | 446 ± 9 |
| **Dendrite size** | 6589 ± 360 | 6364 ± 271 | 6483 ± 261 | 6245 ± 306 |

**Table 1**: Microglia morphological parameters in the CA1, hilus of the hippocampus, PrL of the prefrontal cortex and BLA, in non-surgery controls (n=14-15), surgery controls (n=13-14), acutely J147 treated (n=14-15) and chronically J147 treated (n=14-15) rats. Density is the number of cell bodies per area of interest and multiplied by 10000. Coverage is measured as IBA positive pixels/ area of interest. Microglia cell size, cell body size and dendrites size are expressed in pixels. *: significant difference (P<0.05) compared to control surgery. #: significant difference (P<0.05) compared to non-surgery, + indicated trend (p<0,1) compared to control surgery.

### Plasma cytokines

**IL-1β:** To assess peripheral inflammation IL-1β was assessed after surgery. The AUC from IL-1β plasma concentrations 1, 6 and 24 hours after surgery did not significantly differ between the groups, although J147 treated rats seemed to have a higher IL-1β AUC (Figure 7). At sacrifice, plasma IL-1β concentrations had declined in all surgery groups and were not different from non-surgery controls (40.3±13.9 in control surgery; 65.7±24.5 in acutely J147 treated rats; 99.5±37.9 in chronically J147 treated rats, compared to 39.1±14.8 pg/ml in non-surgery control rats; n=14 for each group).

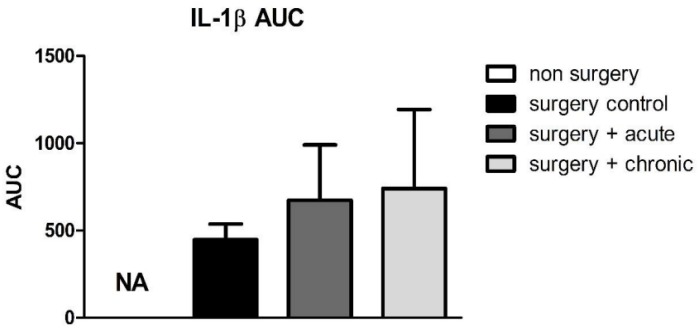


**Figure 7:** Area under the curve (AUC) of 1,6 and 24 hours post-surgery of IL-1β plasma concentrations (mean ± SEM) in the surgery controls (n=14), acutely J147 treated (n=13) and chronically J147 treated (n=14) rats. *: significant difference (P<0.05) between indicated groups.

**Lipocalin:** To further assess inflammation, neutrophil gelatinase-associated lipocalin (NGAL) levels were assessed after surgery and at sacrifice (Figure 8). Plasma collected at 6 hours after surgery from acutely J147 treated rats had a significant higher NGAL concentration than the surgery control rats (Figure 8A). At sacrifice, 14 days after surgery, NGAL was still significantly higher in plasma of the control surgery rats compared to non-surgery rats, but this was not reflected in CSF or hippocampal tissue (Figure 8B and 8C). NGAL concentrations in plasma at sacrifice had declined in all the surgery groups and the difference between the surgery groups waned off, but still was highest in the acutely treated group. No effect of J147 treatment was seen on NGAL concentrations in CSF (Figure 8C), nor on hippocampal NGAL levels (Figure 8D) at the time of sacrifice.

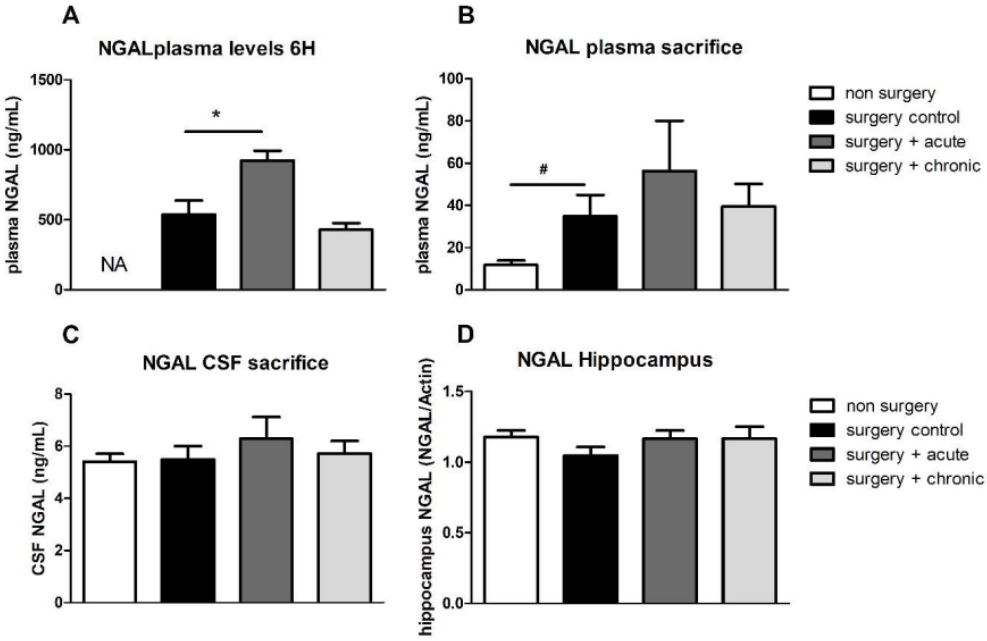


**Figure 8:** Concentrations of neutrophil gelatinase-associated lipocalin (NGAL) (mean ± SEM) in the non-surgery (n=12-14), surgery control (n=11-14), acutely J147 treated (n=12-13) and chronically J147 treated (n=12-15) rats. A) NGAL plasma concentrations 6 hours after surgery (ng/ml), B) NGAL plasma concentrations at sacrifice (14 days after surgery, ng/ml), C) NGAL concentrations in the CSF at sacrifice (ng/ml), and D) NGAL concentrations in the hippocampus at sacrifice (NGAL/actin). *: significant ($p<0.05$) difference between indicated groups (effect of J147 treatment). #: significant ($P<0.05$) effect of surgery.

### Cell metabolism

Cell metabolism in the hippocampus was determined by the phosphorylation of AMPK and rpS6. Ratio of phosphorylated AMPK and AMPK was significant lowered by surgery (Table 2). However, no effect of J147 treatment was seen in ratio of phosphorylated AMPK to total AMPK, or phosphorylated rpS6 to total rpS6 (Table 2). However, hippocampi of chronically treated rats contained more AMPK and rpS6 compared to the control surgery group (Table 2). No difference was seen in the phosphorylated AMPK and rpS6 between the surgery groups (Table 2).

| | Non-Surgery | Control surgery | Surgery + acute J147 | Surgery + chronic J147 |
|---|---|---|---|---|
| AMPK | 0.61 ± 0.03 | 0.70 ± 0 .01 | 0.75 ± 0.08 | 1.18 ± 0.20 * |
| rpS6 | 0.19 ± 0.01 | 0.21 ± 0.02 | 0.26 ± 0.02 | 0.43 ± 0.07 * |
| p-AMPK | 0.20 ± 0.02 +(p=0.052) | 0.15 ± 0.01 | 0.15 ± 0.01 | 0.18 ± 0.01 |
| p-rpS6 | 0.53 ± 0.06 | 0.39 ± 0.04 | 0.39 ± 0.04 | 0.45 ± 0.11 |

| | | | | |
|---|---|---|---|---|
| p-AMPK/AMPK | 0.35 ± 0.03 | 0.23 ± 0.03# | 0.21 ± 0.03 | 0.17 ± 0.03 |
| P-rpS6/rpS6 | 2.59 ± 0.27+(p=0.058) | 1.83 ± 0.25 | 1.53 ± 0.17 | 1.19 ± 0.25+(p=0.051) |

**Table 2:** Cell metabolism measured as (phosphorylated) AMPK and (phosphorylated) rpS6 (Mean ± SEM) in the non-surgery group (n=14-15), the control surgery (n=9-10), acutely J147 treated (n=11-14) and chronically J147 treated rats (8-9). *: significant difference (P<0.05) compared to control surgery. #: significant difference (P<0.05) compared to non-surgery. + indicated trend (p<0,1) compared to control surgery.

## Discussion

### General

The aim of this current study was to explore the therapeutic potential of J147 to prevent POCD in our rat model. Effects of acute and chronic treatment with J147 were studied by assessing cognitive functions, (neuro)inflammation markers, cell metabolism and neurogenesis. Results showed that chronic, but not acute, J147 treatment significantly prevented cognitive dysfunction, as indicated by preserved short and long-term spatial memory. However, neither peripheral-, nor neuroinflammation was affected by either treatment strategy, nor was the surgery-induced reduction of neurogenesis. Similarly, surgery-induced changes in cell metabolism as alternative mechanism were not reversed. Therefore, we conclude that chronic, but not acute J147 treatment can prevent POCD in the rat model, providing a promising novel therapeutic route for POCD therapy in patients. However, the underlying mechanisms need further investigation as the favorable cognitive results seemed not attributable to the anti-inflammatory nor to the cell metabolic effects of J147.

### Effects of J147:

**Post-surgical recovery:** As expected, surgery rats significantly lost body weight, indicating that our abdominal surgery with a jugular vein catheter model had a significant impact on the rats. These results are in accordance with previous findings [27]. Moreover, bodyweight loss seemed a good predictor for cognitive function and neuroinflammation in increased risk conditions, such as aging and infection history [4,28]. The acute J147 treated rats did not differ from the control surgery rats in body weight loss. However, chronic J147 treated animals lost less weight after surgery than the control surgery animals and fully regained their weight within 5 days, indicating a better recovery. Since the reduced body weight loss was not compensated for by increased food intake, this may point to metabolic changes caused by chronic J147 treatment.

**Behavior:** We have extensively studied the time course of behavioral changes after surgery in young healthy Wistar rats before [27]. Results indicated a temporal decline in short-term as well as long-term spatial memory, without affecting open field exploration and short-term object memory. Spatial learning and cognitive flexibility appeared not altered in these young healthy rats, but may become involved in the more wide-spread cognitive dysfunction, when risk factors were added, such as older age [28,55] or infection history [4]. In the current study, general exploratory behavior and anxious/depressive-like behavior were assessed in the OF. Chronic J147 treated animals tended to pay more visits to the center area and displayed more rearings, at similar distance moved, indicating less anxiety at similar exploration. Similarly, Pan et al. showed that mice showed less anxiety in the open field test after treatment with J147 [45]. Lian et al. confirmed this data by showing that J147 treatment could reduce depressive-like behavior in forced swimming- and tail suspension tests, partially through upregulation of the serotonin 1A receptor [42,44]. If indeed chronic J147 rats appear less anxious, this may be generalized, and could contribute to the performance in other behavioral tests outcomes as well. As POCD can affect different brain areas [1], we included different cognitive tests, NOR/ NLR test for short-term object and spatial memory and MWM to assess long-term spatial learning and memory, and cognitive flexibility. Although previous research with acute treatment of J147 showed promising results [43], in the present study acute treatment with J147 did not lead to prevention of cognitive dysfunction. This could be due to the timing of administration or dose level. However, concentration and dose of J147 were carefully chosen to be at their highest during the time of surgery and would be metabolized within 12 hours afterwards (ABREXA, personal communication). On the other hand, chronic treatment with J147, starting one week before surgery until sacrifice, led to completely preserved cognitive performance. The most important outcomes of the study were that chronic J147 treatment restored both short and long-term spatial memory, reflected in the Novel location test and the probe trail of the Morris Water maze. As memory dysfunction is the main symptom of POCD, preventing this aspect is one of the primary aims in POCD research. Our results are in agreement with previous studies that also showed the positive effects of J147 treatment on cognition in dementia models [34,35,37,38]. We cannot exclude an effect of reduced anxiety on cognitive performance in the chronically treated rats [56], since previous studies stress the notion that anxiety and cognition are closely associated and interacting processes. It remains unclear to what extent cognitive (dys)function may precede or result from anxiety [56-59]. Moreover, memory processes and anxiety share involved brain structures, such as the amygdala and hippocampus [60,61]. Nevertheless, cognitive dysfunction, neuroinflammation and

reduced neurogenesis in our control surgery rats appeared without effects on open field behavior, indicating limited effects of anxiety in the development of POCD. In conclusion, the behavioral data show that chronic, but not acute, treatment with J147 can prevent cognitive impairment in our POCD model.

## Mechanisms

**(Neuro)inflammation and neurogenesis:** As short and long-term spatial memory were preserved in the chronic J147 treated animals and (neuro)inflammation is supposed to play a key role in POCD development [6-10], it was anticipated that chronic J147 treated rats would display lower (neuro)inflammation. Although, Cibelli et al, showed that different pro-inflammatory cytokine responses follow different time courses [7], POCD seemed highly associated with IL-1β responses [7,20,27]. Surprisingly, neither early (first 24 hours after surgery), nor later (sacrifice) plasma IL-1β levels indicated reduced peripheral inflammation in chronically J147 treated rats. Similarly, neutrophil gelatinase-associated lipocalin (NGAL) levels, an inflammation marker that in our previous studies was associated with cognitive dysfunction in our POCD model [53] was not reduced by chronic J147 treatment. However, at peak level, 6 hours after surgery [54], plasma NGAL in acute J147 treated animals was significantly elevated, suggesting that administration just before surgery can stimulate lipocalin production up to 6 hours after surgery. At sacrifice, group differences had waned off and plasma, CSF and hippocampal levels were not different between groups. As previously described, neuroinflammation is expected to be elevated 1 week after surgery, subsided in the second week, and became declined at the third week [27], indicating a distinct time course for microglia activation. In this current study the rats were sacrificed 2 weeks after the surgery, which could be the period in which the neuroinflammation was subsiding. It could well be that J147 shifted the time course of the cytokine response, rather than, or in combination with, altering the magnitude. Finally, although a body of evidence indicated an important role of (neuro)inflammation in the development of POCD, a direct causal relationship may not seem evident. Treatment with anti-inflammatory drugs did not always prevent POCD [32], and may even be associated with increased neuroinflammation [33]. This supports the idea that inhibition of inflammation is not sufficient to prevent POCD [32], and other mechanisms may play a role as well.

**mTOR pathway signalling:** Although the design of the present study evaluating the effects of J147 in POCD was mainly focused on anti-inflammatory effects, to touch upon alternative mechanisms, the role of metabolic properties of J147 were also examined. Previous research showed that J147 binds to and partially inhibits the mitochondrial alfa-F1 subunit of ATP synthase (ATP5A). Consequently, J147 can cause an increase in intracellular calcium leading to activation of the AMPK/mTOR pathway, a canonical longevity mechanism [35]. Activation by phosphorylation of AMPK subsequently leads to reduction of unnecessary ATP expenditure by decreasing rpS6 kinase activity through less phosphorylation [35,39-41]. Surprisingly, our data indicated, if anything, a further decline of the surgery-induced lower phosphorylated AMPK to total AMPK and phosphorylated rpS6 and total S6, indicating no difference in activation of AMPK or rpS6. On the other hand, in the chronic J147 treated animals the total AMPK and rpS6 were increased. This is in disagreement with a previous study [35], showing that AMPK decreased and p-AMPK/AMPK ratio increased after long term J147 treatment. Moreover, no correlations between cognitive performance and phosphorylated AMPK to total AMPK and phosphorylated rpS6 and total S6 further supported absence of a direct link between this mechanism and the prevention of POCD by J147 in this study.

## Limitations and future implications

In this study we used a POCD rat model that was established in our lab by Hovens et al. [27]. Although the non-surgery rats seemed to underperform in some of the cognitive tests, effects of surgery, including body weight loss, impaired spatial memory, microglia activation in the hippocampal CA1 area and declined neurogenesis, were in agreement with our previous studies [27,33]. Therefore, we conclude that the abdominal surgery rats provided a relevant model to explore potential therapeutic effects of J147. To focus on the main aim of the study, evaluating potential therapeutic properties of J147 in POCD, we analyzed effects of treatment independent of the non-surgery group. In the present study we used healthy young Wister rats. The major risk factors for POCD are older age and pre-operative health. Therefore, young healthy Wister rats may not provide the best representative of the general elderly patients population that develop POCD. On the other hand, results in these young healthy rats provided a relevant contribution to unravelling the mechanism of POCD. Given the promising effects of J147 in this young rat POCD model, the logical next step would involve studies in an animal model presenting one or more of the human risk factors for developing POCD. J147 treatment was given at one dose and at specific time slots. Although chosen carefully, regarding the time course of cognitive decline and that of the (neuro)inflammatory response [27], timing could provide a relevant target for further optimization and may help to better understand the pathophysiology of POCD and therapeutic options.

## Conclusion

As the profile of J147 included anti-dementia and anti-inflammatory effects, the present study investigated the therapeutical potential of J147 in a rat model for POCD. Chronic, but not acute treatment with J147 significantly preserved behavioral and cognitive performance in our rat model for POCD. Although (neuro)inflammation may play a key role in the development of POCD, prevention by J147 could not be attributed to anti-

inflammatory effects, nor to cell-metabolic effect of J147. Since cognitive decline is the key feature of human POCD, the finding that J147 preserves cognition in our POCD model indicates that J147 may provide a novel therapeutic route in the treatment of clinical POCD. The underlying mechanisms, though, need further investigation.

## References


1. I. B. Hovens, R. G. Schoemaker, E. A. van der Zee, E. Heineman, G. J. Izaks, et al. (2012) Thinking through postoperative cognitive dysfunction: How to bridge the gap between clinical and pre-clinical perspectives, (in eng), Brain Behav Immun 26: 1169-1179.
2. C. C. Price, C. W. Garvan, T. G. Monk (2008) Type and severity of cognitive decline in older adults after noncardiac surgery, (in eng), Anesthesiology 108: 8-17.
3. T. G. Monk (2008) Predictors of cognitive dysfunction after major noncardiac surgery, (in eng), Anesthesiology 1: 18-30.
4. I. B. Hovens, B. L. van Leeuwen, C. Nyakas, E. Heineman, E. A. van der Zee, et al. (2015) Schoemaker, Prior infection exacerbates postoperative cognitive dysfunction in aged rats, (in eng), Am J Physiol Regul Integr Comp Physiol 309: 148-159.
5. M. Plas (2017) Cognitive decline after major oncological surgery in the elderly, (in eng), Eur J Cancer 86: 394-402.
6. L. Krenk, L. S. Rasmussen, H. Kehlet (2010) New insights into the pathophysiology of postoperative cognitive dysfunction, (in eng), Acta Anaesthesiol Scand 54: 951-956.
7. M. Cibelli (2010) Role of interleukin-1beta in postoperative cognitive dysfunction, (in eng), Ann Neurol 68: 360-368.
8. L. Peng, L. Xu, W. Ouyang (2013) Role of peripheral inflammatory markers in postoperative cognitive dysfunction (POCD): a meta-analysis, (in eng), PLoS One 8: 79624.
9. N. Terrando, C. Monaco, D. Ma, B. M. Foxwell, M. Feldmann, et al. (2010) Tumor necrosis factor-alpha triggers a cytokine cascade yielding postoperative cognitive decline, (in eng), Proc Natl Acad Sci U S A 104: 20518-20522.
10. A. E. van Harten, T. W. Scheeren, A. R. Absalom (2012) A review of postoperative cognitive dysfunction and neuroinflammation associated with cardiac surgery and anaesthesia, (in eng), Anaesthesia 67: 280-293.
11. D. R. Skvarc (2018) Post-Operative Cognitive Dysfunction: An exploration of the inflammatory hypothesis and novel therapies, (in eng), Neurosci Biobehav Rev 84: 116-133.
12. X. Lin, Y. Chen, P. Zhang, G. Chen, Y. Zhou, X. Yu (2020) The potential mechanism of postoperative cognitive dysfunction in older people, (in eng), Exp Gerontol 130.
13. B. Ramlawi (2006) C-Reactive protein and inflammatory response associated to neurocognitive decline following cardiac surgery, (in eng), Surgery 140: 221-226.
14. Y. Beloosesky et al (2007) Cytokines and C-reactive protein production in hip-fracture-operated elderly patients, (in eng), J Gerontol A Biol Sci Med Sci 62: 420-426.
15. K. Yaffe (2003) Inflammatory markers and cognition in well-functioning African-American and white elders, (in eng), Neurology 61: 76-80.
16. R. N. Dilger, R. W. Johnson (2008) Aging, microglial cell priming, and the discordant central inflammatory response to signals from the peripheral immune system, (in eng), J Leukoc Biol 84: 932-939.
17. Y. Wan, J. Xu, D. Ma, Y. Zeng, M. Cibelli, et al. (2007) Postoperative impairment of cognitive function in rats: a possible role for cytokine-mediated inflammation in the hippocampus, (in eng), Anesthesiology 106: 436-443.
18. J. X. Tang, D. Baranov, M. Hammond, L. M. Shaw, M. F. Eckenhoff, et al. (2011) Human Alzheimer and inflammation biomarkers after anesthesia and surgery, (in eng), Anesthesiology 115: 727-732.
19. R. Yirmiya, I. Goshen (2011) Immune modulation of learning, memory, neural plasticity and neurogenesis, (in eng), Brain Behav Immun 25: 181-213.
20. R. M. Barrientos, A. M. Hein, M. G. Frank, L. R. Watkins, S. F. Maier (2012) Intracisternal interleukin-1 receptor antagonist prevents postoperative cognitive decline and neuroinflammatory response in aged rats, (in eng), J Neurosci 32: 14641-14648.
21. P. Jiang, Q. Ling, H. Liu, W. Tu (2015) Intracisternal administration of an interleukin-6 receptor antagonist attenuates surgery-induced cognitive impairment by inhibition of neuroinflammatory responses in aged rats, (in eng), Exp Ther Med 9: 982-986.
22. A. R. Kamer (2012) Meloxicam improves object recognition memory and modulates glial activation after splenectomy in mice, (in eng), Eur J Anaesthesiol 29: 332-337.
23. J. Hu (2018) Interleukin-6 is both necessary and sufficient to produce perioperative neurocognitive disorder in mice, (in eng), Br J Anaesth 120: 537-545.
24. Y. Z. Zhu, R. Yao, Z. Zhang, H. Xu, L. W. Wang (2016) Parecoxib prevents early postoperative cognitive dysfunction in elderly patients undergoing total knee arthroplasty: A double-blind, randomized clinical consort study, (in eng), Medicine (Baltimore) 95.
25. Y. Zhu (2018) Protective Effect of Celecoxib on Early Postoperative Cognitive Dysfunction in Geriatric Patients, (in eng), Front Neurol 9: 633.
26. L. S. Valentin (2016) Effects of Single Low Dose of Dexamethasone before Noncardiac and Nonneurologic Surgery and General Anesthesia on Postoperative Cognitive Dysfunction-A Phase III Double Blind, Randomized Clinical Trial, (in eng), PLoS One 11.
27. I. B. Hovens, R. G. Schoemaker, E. A. van der Zee, A. R. Absalom, E. Heineman, et al. (2014) Postoperative cognitive dysfunction: Involvement of neuroinflammation and neuronal functioning, (in eng), Brain Behav Immun 38: 202-210.
28. I. B. Hovens, R. G. Schoemaker, E. A. van der Zee, E. Heineman, C. Nyakas, et al. (2013) Surgery-induced behavioral changes in aged rats, (in eng), Exp Gerontol 48: 1204-1211.
29. R. M. Barrientos (2006) Peripheral infection and aging interact to impair hippocampal memory consolidation, (in eng), Neurobiol Aging 27: 723-732.
30. J. A. Hudetz, K. M. Patterson, O. Amole, A. V. Riley, P. S. Pagel (2011) Postoperative cognitive dysfunction after noncardiac surgery: effects of metabolic syndrome, (in eng), J Anesth 25: 337-344.
31. X. Su (2013) Dysfunction of inflammation-resolving pathways is associated with exaggerated postoperative cognitive decline in a rat model of the metabolic syndrome, (in eng), Mol Med 18: 1481-1490.

**32.** F. Mohammadian, M. A. Firouzjaei, M. Haghani, M. Shabani, S. M. Shid Moosavi, et al. (2019) Inhibition of inflammation is not enough for recovery of cognitive impairment in hepatic encephalopathy: Effects of minocycline and ibuprofen, (in eng), Brain Res Bull 149: 96-105.

**33.** K. Oberman, I. Hovens, J. de Haan, J. Falcao-Salles, B. van Leeuwen, et al. (2021) Acute pre-operative ibuprofen improves cognition in a rat model for postoperative cognitive dysfunction, (in eng), J Neuroinflammation 18.

**34.** A. Currais (2019) Elevating acetyl-CoA levels reduces aspects of brain aging, (in eng), Elife 8.

**35.** J. Goldberg (2018) The mitochondrial ATP synthase is a shared drug target for aging and dementia, (in eng), Aging Cell 17.

**36.** J. Goldberg (2020) Targeting of intracellular Ca, (in eng), NPJ Aging Mech Dis 6.

**37.** M. Prior, R. Dargusch, J. L. Ehren, C. Chiruta, D. Schubert (2013) The neurotrophic compound J147 reverses cognitive impairment in aged Alzheimer's disease mice, (in eng), Alzheimers Res Ther 5: 25.

**38.** M. Prior (2016) Selecting for neurogenic potential as an alternative for Alzheimer's disease drug discovery, (in eng), Alzheimers Dement 12: 678-686.

**39.** A. Currais (2015) A comprehensive multiomics approach toward understanding the relationship between aging and dementia, (in eng), Aging (Albany NY) 7: 937-955.

**40.** I. A. Emmanuel, F. Olotu, C. Agoni, M. E. S. Soliman (2019) Broadening the horizon: Integrative pharmacophore-based and cheminformatics screening of novel chemical modulators of mitochondria ATP synthase towards interventive Alzheimer's disease therapy, (in eng), Med Hypotheses 130.

**41.** J. W. Larrick, A. R. Mendelsohn (2018) ATP Synthase, a Target for Dementia and Aging?, (in eng), Rejuvenation Res 21: 61-66.

**42.** L. Lian (2018) Antidepressant-like effects of a novel curcumin derivative J147: Involvement of 5-HT, (in eng), Neuropharmacology 135: 506-513.

**43.** D. J. Daugherty, A. Marquez, N. A. Calcutt, D. Schubert (2018) A novel curcumin derivative for the treatment of diabetic neuropathy, (in eng), Neuropharmacology 129: 26-35.

**44.** J. Li (2020) Sub-Acute Treatment of Curcumin Derivative J147 Ameliorates Depression-Like Behavior Through 5-HT, (in eng), Front Neurosci 14: 701.

**45.** X. Pan (2021) Activation of monoaminergic system contributes to the antidepressant- and anxiolytic-like effects of J147, (in eng), Behav Brain Res 411.

**46.** R. G. Schoemaker, J. F. Smits (1994) Behavioral changes following chronic myocardial infarction in rats, (in eng), Physiol Behav 56: 585-589.

**47.** R. Morris (1984) Developments of a water-maze procedure for studying spatial learning in the rat, (in eng), J Neurosci Methods 11: 47-60.

**48.** I. B. Hovens, C. Nyakas, R. G. Schoemaker (2014) A novel method for evaluating microglial activation using ionized calcium-binding adaptor protein-1 staining: cell body to cell size ratio, Neuroimmunology and Neuroinflammation 1: 82-88.

**49.** G. W. Kreutzberg (1996) Microglia: a sensor for pathological events in the CNS, (in eng), Trends Neurosci 19: 312-318.

**50.** M. Augusto-Oliveira, G. P. Arrifano, C. I. Delage, M. Tremblay, M. E. Crespo-Lopez, et al. (2021) Plasticity of microglia, (in eng), Biol Rev Camb Philos Soc 2021.

**51.** S. Chakraborty, S. Kaur, S. Guha, S. K. Batra (2012) The multifaceted roles of neutrophil gelatinase associated lipocalin (NGAL) in inflammation and cancer, (in eng), Biochim Biophys Acta 1826.

**52.** P. J. Naudé (2014) Sex-specific associations between Neutrophil Gelatinase-Associated Lipocalin (NGAL) and cognitive domains in late-life depression, (in eng), Psychoneuroendocrinology 48: 169-177.

**53.** L. Gouweleeuw, I. B. Hovens, B. L. van Leeuwen, R. G. Schoemaker (2017) Neutrophil gelatinase-associated lipocalin and microglial activity are associated with distinct postoperative behavioral changes in rats, (in eng), Behav Brain Res 319: 104-109.

**54.** I. B. Hovens, B. L. van Leeuwen, M. A. Mariani, A. D. Kraneveld, R. G. Schoemaker (2016) Postoperative cognitive dysfunction and neuroinflammation; Cardiac surgery and abdominal surgery are not the same, (in eng), Brain Behav Immun 54: 178-193.

**55.** I. B. Hovens, B. L. van Leeuwen, C. Nyakas, E. Heineman, E. A. van der Zee, et al. (2015) Postoperative cognitive dysfunction and microglial activation in associated brain regions in old rats, (in eng), Neurobiol Learn Mem 118: 74-79.

**56.** A. R. Salomons, S. S. Arndt, F. Ohl (2012) Impact of anxiety profiles on cognitive performance in BALB/c and 129P2 mice, (in eng), Cogn Affect Behav Neurosci 12: 794-803.

**57.** M. Garner, H. Möhler, D. J. Stein, T. Mueggler, D. S. Baldwin (2009) Research in anxiety disorders: from the bench to the bedside, (in eng), Eur Neuropsychopharmacol 19: 381-390.

**58.** A. Beuzen, C. Belzung (1995) Link between emotional memory and anxiety states: a study by principal component analysis, (in eng), Physiol Behav 58: 111-118.

**59.** N. McNaughton (1997) Cognitive dysfunction resulting from hippocampal hyperactivity--a possible cause of anxiety disorder?, (in eng), Pharmacol Biochem Behav 56: 603-611.

**60.** E. Engin, D. Treit (2007) The role of hippocampus in anxiety: intracerebral infusion studies, (in eng), Behav Pharmacol 18: 365-374.

**61.** J. E. LeDoux (2018) Emotion circuits in the brain, (in eng), Annu Rev Neurosci 23: 155-184.